

J.C. Hubbert\*, G. Meymaris and M. Dixon

National Center for Atmospheric Research, Boulder, CO

## 1. INTRODUCTION

Phase coding of the radar transmit pulses can be used to mitigate range overlaid echoes. SZ phase coding uses a systematic phase coding scheme which has been employed by the NEXRAD radars (Sachidananda and Zrnić 1999). Phase coding for dual polarization radars was investigated by Bharadwaj and Chandrasekar (2007) who examined and compared both SZ and random phase coding for simultaneous transmission of H and V polarizations where both H and V channels were modulated with the same phase code. Here we examine SZ phase coding for fast alternating H and V transmission radars such as S-Pol, NCAR’s dual polarimetric research radar. Specifically we investigate using separate phase codes for the H and V channels.

When the transmit pulses are phase coded, overlaid echoes from different trips will have different phase codes. In order to “receive” a particular trip echo, the phase code for that trip is subtracted from the corresponding samples. The other “out-of-trip” echoes are modulated and those resulting phases are termed modulation codes. The modulation codes cause the echoes to be spread across the spectrum so that they mimic white noise. Thus, these overlaid powers do not bias the velocity estimates from the cohered signal. Phase coding to extend the unambiguous range of dual polarization radars that use the fast alternating H and V polarization transmission technique are described.

## 2. ALTERNATE H AND V TRANSMIT

Phase coding for fast alternating transmission of H and V pulses (FHV) is more complicated than single polarization radar or simultaneous H and V transmission (SHV). There are four received signals, two copolar and two crosspolar. Additionally, second trip echoes appear in the crosspolar channel of the other copolar signal. Bharadwaj and Chandrasekar (2007) showed that if the H and V transmit pulses use the same phase code, estimates of the dual polarization variables that depend on the cross correlation of the H and V channel signals, can be biased.

To avoid this, we propose using a separate phase code for the H and V transmit pulses.

A block diagram of the four time series,  $HH_i$ ,  $VH_i$ ,  $VV_i$  and  $HV_i$ , for a single resolution volume with no overlay is shown in Fig. 1. The proposed transmit pulse train for FHV radar is shown in Fig. 2. The H and V polarized pulses are at equi-spaced intervals. The H pulses are phase coded with  $a_i$  while the V pulses are phase coded with  $c_i$  where  $a_i$  and  $c_i$  are some systematic switching code (Sachidananda and Zrnić 1999). Fig. 3 illustrates the resulting multiple trip echoes and attached phase codes as they would occur for the H and V copolar signals. Second trip echoes come from the previously transmitted V (H) pulse ( $HV_{i-1}c_{i-1}$  (and  $VH_i a_i$ )) and thus are a crosspolar echoes. The third trip echo comes from the previously transmitted H (V) pulse. For the crosspolar channels, the situation is opposite; the second trip echoes are copolar. The copolar H signal can be expressed:

$$R_{CO}^H = HH_i a_i + HV_{i-1}^{2nd} c_{i-1} + HH_{i-1}^{3rd} a_{i-1} + HV_{i-2}^{4th} c_{i-2} \quad (1)$$

where the superscripts indicate the “trip” of the signal and

$$a_i = e^{-j\psi_i}, \quad c_i = e^{-j\theta_i}, \quad (2)$$

are the switching codes. Similarly, the other copolar and crosspolar signals can be expressed,

$$R_X^H = VH_i a_i + VV_{i-1}^{2nd} c_{i-1} + VH_{i-1}^{3rd} a_{i-1} + VV_{i-2}^{4th} c_{i-2} \quad (3)$$

$$R_{CO}^V = VV_i c_i + VH_i^{2nd} a_i + VV_{i-1}^{3rd} c_{i-1} + VH_{i-1}^{4th} a_{i-1} \quad (4)$$

$$R_X^V = HV_i c_i + HH_i^{2nd} a_i + HV_{i-1}^{3rd} c_{i-1} + HH_{i-1}^{4th} a_{i-1} \quad (5)$$

The SZ(n/M) switching code is (code applied to transmit pulses)

$$a_k = \exp \left[ -j \sum_{m=0}^k (n\pi m^2 / M) \right] \quad (6)$$

for  $k = 0, 1, 2 \dots M - 1$ . The SZ(n/M) switching phases are

$$\psi_k = - \sum_{m=0}^k \frac{n\pi m^2}{M} \quad (7)$$

\*NCAR/EOL, Boulder, Colorado 80307, email: hubbert@ucar.edu

The modulation phase then is

$$\phi_k = \psi_{k-t} - \psi_k = \frac{n\pi}{M} \sum_{l=0}^{t-1} (k-l)^2 \quad (8)$$

where  $t$  is the integer delay of the switching code. For SZ(8/64) reported in Sachidananda and Zrnić (1999) the modulation code for  $t = 1$  (second trip echo) is

$$\phi_k^{2^{nd} \text{ trip}} = \psi_{k-1} - \psi_k = \frac{8\pi k^2}{64} = \frac{\pi}{8} k^2 \quad (9)$$

### 3. SZ FOR S-POL WITH PRT = 1 ms

If the PRT between the H and V pulses is 1 ms (or greater), the 4<sup>th</sup> trip begins at 450 km (or more) and thus this 4<sup>th</sup> trip can be neglected. For a radar elevation angle of 0.5° at 450 km range, the radar resolution volume is at about 16 km AGL. This then simplifies the received time series: the received signals then are,

$$R_{CO}^H = HH_i a_i + HV_{i-1}^{2^{nd}} c_{i-1} + HH_{i-1}^{3^{rd}} a_{i-1} \quad (10)$$

$$R_X^H = VH_i a_i + VV_{i-1}^{2^{nd}} c_{i-1} + VH_{i-1}^{3^{rd}} a_{i-1} \quad (11)$$

$$R_{CO}^V = VV_i c_i + VH_i^{2^{nd}} a_i + VV_{i-1}^{3^{rd}} c_{i-1} \quad (12)$$

$$R_X^V = HV_i c_i + HH_i^{2^{nd}} a_i + HV_{i-1}^{3^{rd}} c_{i-1} \quad (13)$$

Cohering to the first trip yields,

$$R_{CO}^{H(1)} = HH_i + HV_{i-1}^{2^{nd}} c_{i-1} a_i^* + HH_{i-1}^{3^{rd}} a_{i-1} a_i^* \quad (14)$$

$$R_X^{H(1)} = VH_i + VV_{i-1}^{2^{nd}} c_{i-1} a_i^* + VH_{i-1}^{3^{rd}} a_{i-1} a_i^* \quad (15)$$

$$R_{CO}^{V(1)} = VV_i + VH_i^{2^{nd}} a_i c_i^* + VV_{i-1}^{3^{rd}} c_{i-1} c_i^* \quad (16)$$

$$R_X^{V(1)} = HV_i + HH_i^{2^{nd}} a_i c_i^* + HV_{i-1}^{3^{rd}} c_{i-1} c_i^* \quad (17)$$

Cohering to the second trip yields,

$$R_{CO}^{H(2)} = HH_i a_i c_{i-1}^* + HV_{i-1}^{2^{nd}} + HH_{i-1}^{3^{rd}} a_{i-1} c_{i-1}^* \quad (18)$$

$$R_X^{H(2)} = VH_i a_i c_{i-1}^* + VV_{i-1}^{2^{nd}} + VH_{i-1}^{3^{rd}} a_{i-1} c_{i-1}^* \quad (19)$$

$$R_{CO}^{V(2)} = VV_i c_i a_i^* + VH_i^{2^{nd}} + VV_{i-1}^{3^{rd}} c_{i-1} a_i^* \quad (20)$$

$$R_X^{V(2)} = HV_i c_i a_i^* + HH_i^{2^{nd}} + HV_{i-1}^{3^{rd}} c_{i-1} a_i^* \quad (21)$$

Cohering to the third trip yields,

$$R_{CO}^{H(3)} = HH_i a_i a_{i-1}^* + HV_{i-1}^{2^{nd}} c_{i-1} a_{i-1}^* + HH_{i-1}^{3^{rd}} \quad (22)$$

$$R_X^{H(3)} = VH_i a_i a_{i-1}^* + VV_{i-1}^{2^{nd}} c_{i-1} a_{i-1}^* + VH_{i-1}^{3^{rd}} \quad (23)$$

Table 1:  $H$  transmit: Modulation code when cohering to trip 1, 2 or 3. ‘0’ indicates that that trip is coherent, i.e., the coherent trip is the strong trip.

$R_{CO}^H, R_X^H$ switching phases			
Trip	$a_i$	$c_{i-1}$	$a_{i-1}$
1	0	$c_{i-1} a_i^*$	$a_{i-1} a_i^*$
2	$a_i c_{i-1}^*$	0	$a_{i-1} c_{i-1}^*$
3	$a_i a_{i-1}^*$	$c_{i-1} a_{i-1}^*$	0

$$R_{CO}^{V(3)} = VV_i c_i c_{i-1}^* + VH_i^{2^{nd}} a_i c_{i-1}^* + VV_{i-1}^{3^{rd}} \quad (24)$$

$$R_X^{V(3)} = HV_i c_i c_{i-1}^* + HH_i^{2^{nd}} a_i c_{i-1}^* + HV_{i-1}^{3^{rd}} \quad (25)$$

where “\*” denotes conjugation. As can be seen in Eqs.(10–25), there are several cross modulation codes that occur when cohering to first, second and third trip echoes. However, there are only two unique modulation codes,

$$code1 = c_i a_i^* \quad (26)$$

$$code2 = c_{i-1} a_i^*. \quad (27)$$

These modulation codes are,

$$c_k a_k^* = - \sum_{m=0}^k \frac{n_c \pi m^2}{M} + \sum_{m=0}^k \frac{n_a \pi m^2}{M} \quad (28)$$

$$= \sum_{m=0}^k \frac{(n_a - n_c) \pi m^2}{M} \quad (29)$$

and,

$$c_{k-1} a_k^* = - \sum_{m=0}^{k-1} \frac{n_c \pi m^2}{M} + \sum_{m=0}^k \frac{n_a \pi m^2}{M} \quad (30)$$

$$= \sum_{m=0}^{k-1} \frac{(n_a - n_c) \pi m^2}{M} + \frac{n_a \pi k^2}{M} \quad (31)$$

The modulation codes are given in Table 1 for for  $R_{CO}^H$  and  $R_X^H$  and Table 2 gives the modulation codes for  $R_{CO}^V$  and  $R_X^V$ .

## 4. SIMULATIONS

SZ(16/128) was investigated for super resolution data by Hubbert et al. (2006) for a PRT of 780 $\mu$ s. The statistics here for the suggested dual polarization SZ(16/128) will be significantly different with the PRT at 2 ms (for just the H or just the V pulse trains). Torres and Zrnić (2009) evaluated generalized SZ( $n$ /64) (for  $0 < n < 64$ ) and

Table 2:  $V$  transmit: Modulation code when cohering to trip 1, 2 or 3. ‘0’ indicates that that trip is coherent, i.e., the coherent trip is the strong trip.

$R_{CO}^V, R_X^V$ switching phases			
Trip	$c_i$	$a_i$	$c_{i-1}$
1	0	$a_i c_i^*$	$c_{i-1} c_i^*$
2	$c_i a_i^*$	0	$c_{i-1} a_i^*$
3	$c_i c_{i-1}^*$	$a_i c_{i-1}^*$	0

found acceptable recovery performance for many values of  $n$ . Based on their work, we expect SZ(15/128) to perform similarly to SZ(16/128).

To our knowledge, no one has simulated FHV dual polarization scheme that uses two different switching codes. As shown above modulation codes are created that are a combination of the two switching codes. We have not performed an exhaustive evaluation but we did find that if the two used switching codes had a difference of one, i.e.,  $|n_1 - n_2| = 1$  for SZ( $n_1$ /128) and SZ( $n_2$ /128), the recovery statistics were in general better as compared to other  $n_1 - n_2$  differences.

We first examine the power spectra of the modulation codes for a switching code lag of 1. This then is the modulation codes for the copolar third trip echoes and the cross-modulation code resulting from SZ(16/128) (strong trip) and SZ(15/128) (weak trip). Fig. 4 shows the power spectra of the modulation codes in the left column. The right column shows the corresponding power spectra after the modulations codes have been filtered with a 0.625 spectrum width notch, inversed FFT’d, cohered for the “weak trip” and then FFT’d again to obtain the power spectrum. The plots due to SZ(15/128) and SZ(16/128)-SZ(15/128) are significantly different from the plots due to SZ(16/128). It quite interesting that the SZ(16/128)-SZ(15/128) power spectrum after notching (lower right panel) contains only one spectral “spike”. The underlying weak trip signal spectrum is convolved with this spectrum to create the SZ-processed weak signal spectrum. Thus there is only one “replica spectrum” for this case.

Some of the recovery statistics according to the above modulations codes are presented next. In general, the wavelength is 10.68 cm, PRT=2 ms, 128 samples, phase noise is modeled as  $\pm 0.25^\circ$  (uniform random),  $\rho_{hv} = 0.99$ ,  $Z_{dr} = 2$  dB, the horizontal axis is strong trip spectrum width, and the vertical axis is the strong trip to weak trip power ratio. Fig. 5 shows the standard deviation (SD) of the weak trip velocity for SZ(16/128) (left) and for SZ(15/128) (right), both for a weak trip spectrum width of  $2 \text{ m s}^{-1}$ . The recovery statistics are similar to SZ(8/64) for a PRT of roughly 1 ms except the horizontal axis has been compressed by about a factor of 2 since the PRT

here is 2 ms. Thus, wide spectrum width signals are not recovered nearly as well here.

Figure 6 shows the SD of the weak trip velocity for SZ(16/128)-SZ(15/128). The left panel is for a weak trip SW of  $2 \text{ m s}^{-1}$  and the right panel is for a weak trip SW of  $4 \text{ m s}^{-1}$ . Figure 7 show the bias for weak trip power. Figure 8 show the bias and SD for strong trip  $Z_{dr}$  while Fig. 9 show he bias and SD for strong trip  $\phi_{dp}$ .

## 5. CONCLUSIONS

This paper addressed SZ phase coding for FHV dual polarization radar. To avoid multiple trip echoes that would be correlated (as discussed in Bharadwaj and Chandrasekar (2007)) the H and V pulses were gives different switching phase codes: SZ(16/128) for H and SZ(15/128) for V. The preliminary statistical performance plots indicate that the scheme will work reasonably well. Using a PRT=2 ms does limit the recovery area as compared to previously reported SZ(8/64) (Sachidananda and Zrnić 1999). This new phase coding scheme will be implemented on S-Pol which typically uses a PRT of 1 ms between the H and V pulses and thus first trip data is restricted to 150 km with no mitigation for multiple trip echoes. Thus we expect this scheme to significantly improve S-Pol data quality.

### Acknowledgment

The NCAR S-Pol is supported by the National Science Foundation. Any opinions, findings and conclusions or recommendations expressed in this publication are those of the authors and do not necessarily reflect the views of the National Science Foundation.

## References

- Bharadwaj, N. and V. Chandrasekar, 2007: Phase coding for range ambiguity mitigation in dual-polarized Doppler weather radars. *J. Atmos. Oceanic Technol.*, **24**, 1351–1363.
- Hubbert, J., G. Meymaris, S. Ellis, and M. Dixon: 2006, Application and issues of SZ phase coding for NEXRAD. *Proceedings of 22<sup>th</sup> International Conference on IIPS*, Amer. Meteor. Soc., Atlanta, GA, volume 87<sup>th</sup> Annual Meeting.
- Sachidananda, M. and D. Zrnić, 1999: Systematic phase codes for resolving range overlaid signals in a Doppler weather radar. *J. Atmos. Oceanic Technol.*, **16**, 1351–1363.

Torres, S. and D. Zrić: 2009, Generalized SZ phase codes to mitigate range and velocity ambiguities. *Preprints, 34<sup>th</sup> AMS Conf. on Radar Meteorology*, AMS, Williamsburg, VA.

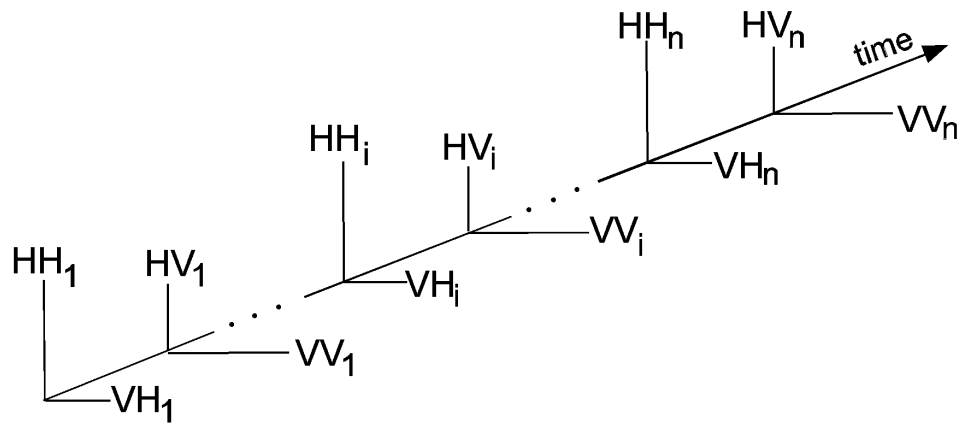


Figure 1: *The received time series for dual polarization radar.*

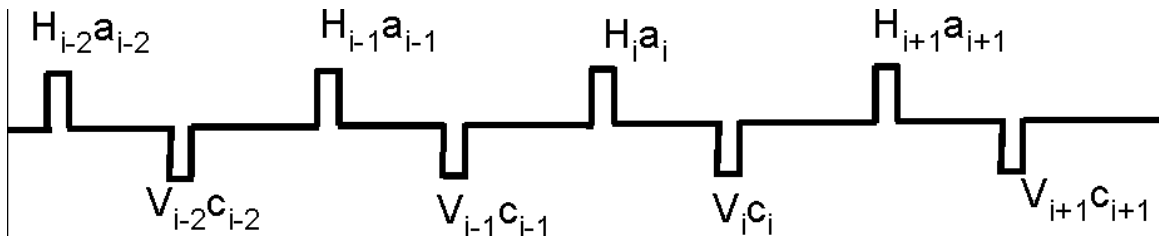


Figure 2: *Transmit pulse train for phase coded FHV dual polarization radar.*

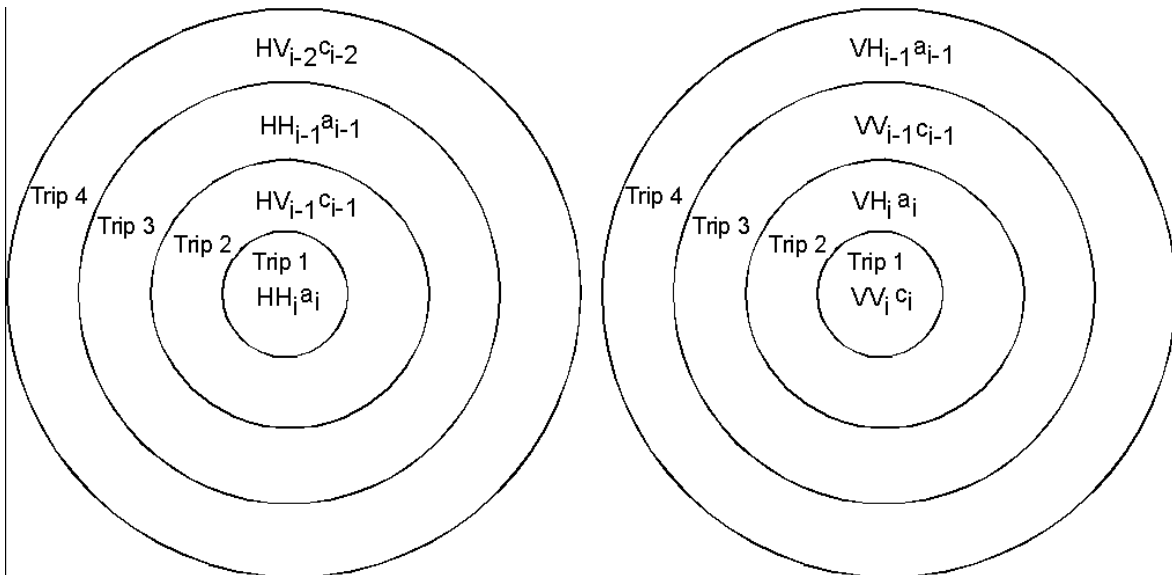


Figure 3: *The trip rings and overlaid echoes for FHV dual polarization.*

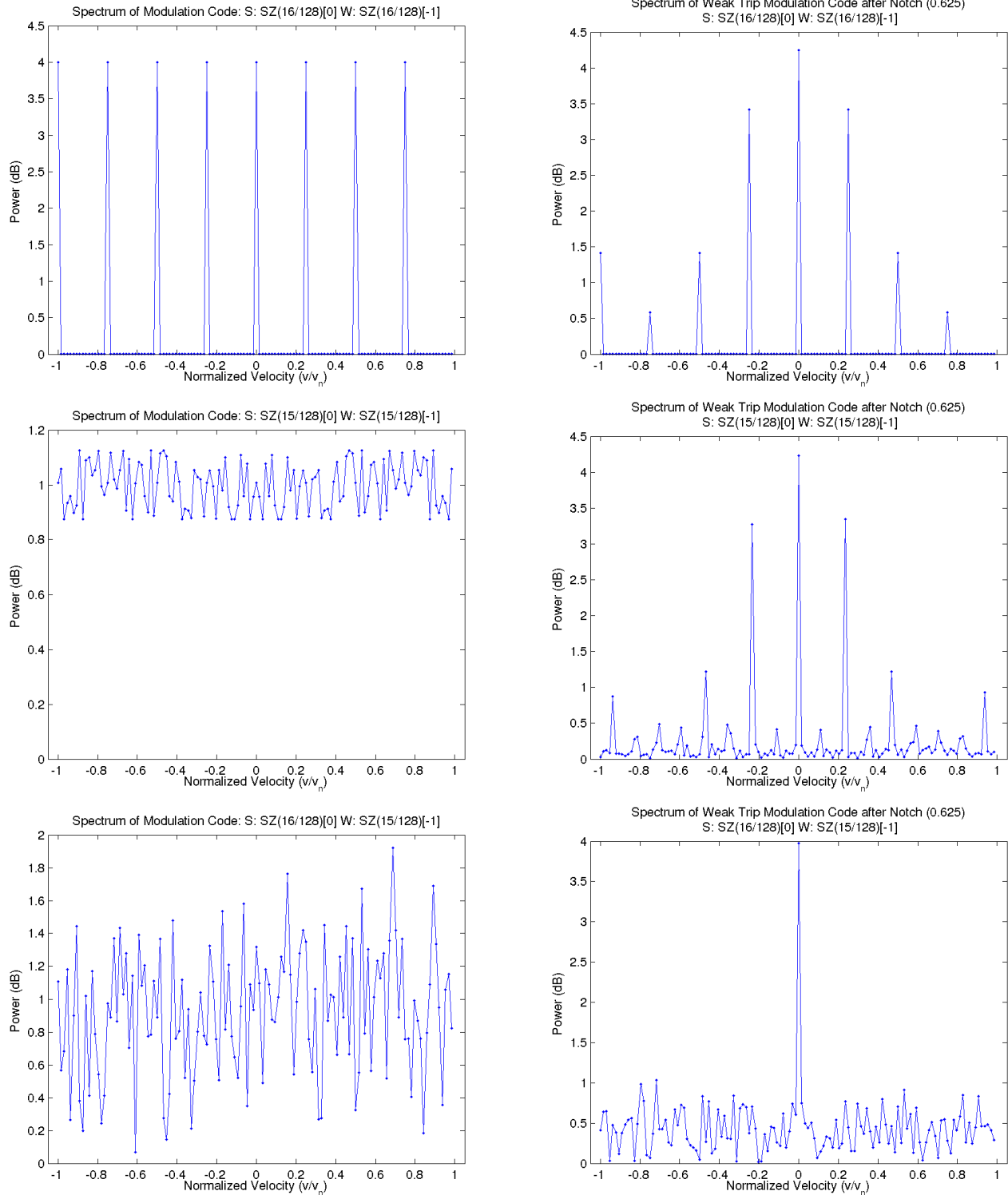
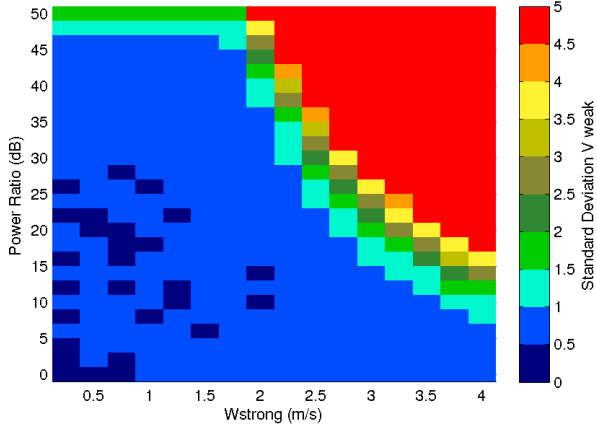


Figure 4: Spectra of modulation codes. Top to bottom rows: SZ(16/128) (lag-1), SZ(15/128) (lag-1), SZ(16/128)-SZ(15/128) (lag-1). Left column: power spectrum of modulation code. Right column: power spectrum after a 0.625 spectrum width notch filter, cohering to the “weak trip” and again calculating the power spectrum.

Standard Deviation V weak:  $\lambda=10.68\text{cm}$ ,  $T_s=1.0\text{ms}$ ,  $N=128$ , Phase Noise= $\pm 0.25^\circ$   
 Trip 1 [CO, Zdr=2,  $\rho_{HV}=0.99$ ,  $W=2$ ], Trip 2 [Cross,  $\rho_{HV}=0.99$ ]  
 H: SZ(16/128), V: SZ(16/128), SZ: 2 trip, PNF=0.625



Standard Deviation V weak:  $\lambda=10.68\text{cm}$ ,  $T_s=1.0\text{ms}$ ,  $N=128$ , Phase Noise= $\pm 0.25^\circ$   
 Trip 1 [CO, Zdr=2,  $\rho_{HV}=0.99$ ,  $W=2$ ], Trip 2 [Cross,  $\rho_{HV}=0.99$ ]  
 H: SZ(15/128), V: SZ(15/128), SZ: 2 trip, PNF=0.625

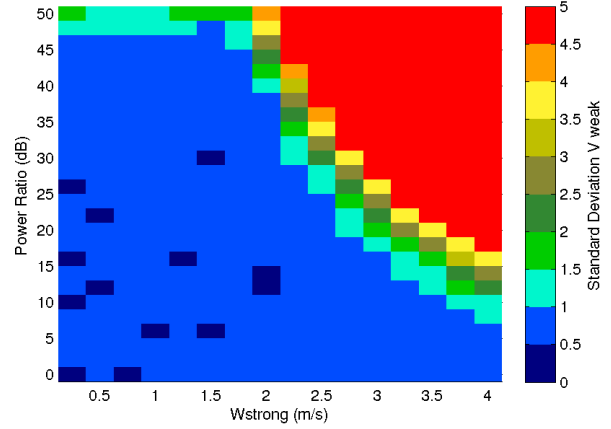
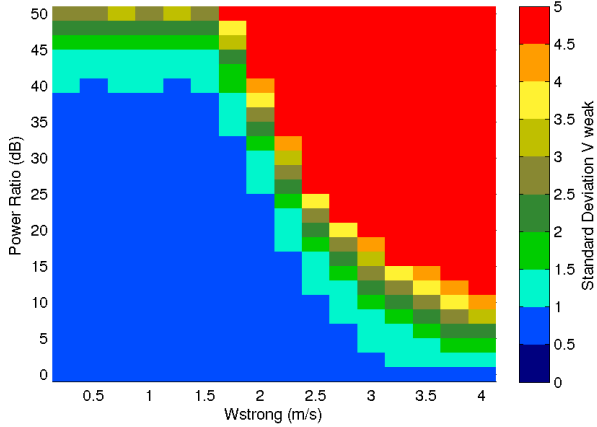


Figure 5: Standard deviation for weak trip velocity for SZ(16/128) (left) and SZ(15/128) (right). PRT=2 ms, 128 samples, weak trip spectrum width is  $2\text{ m s}^{-1}$ .

Standard Deviation V weak:  $\lambda=10.68\text{cm}$ ,  $T_s=1.0\text{ms}$ ,  $N=128$ , Phase Noise= $\pm 0.25^\circ$   
 Trip 1 [CO, Zdr=2,  $\rho_{HV}=0.99$ ,  $W=2$ ], Trip 2 [Cross,  $\rho_{HV}=0.99$ ]  
 H: SZ(16/128), V: SZ(15/128), SZ: 2 trip, PNF=0.625



Standard Deviation V weak:  $\lambda=10.68\text{cm}$ ,  $T_s=1.0\text{ms}$ ,  $N=128$ , Phase Noise= $\pm 0.25^\circ$   
 Trip 1 [CO, Zdr=2,  $\rho_{HV}=0.99$ ,  $W=4$ ], Trip 2 [Cross,  $\rho_{HV}=0.99$ ]  
 H: SZ(16/128), V: SZ(15/128), SZ: 2 trip, PNF=0.625

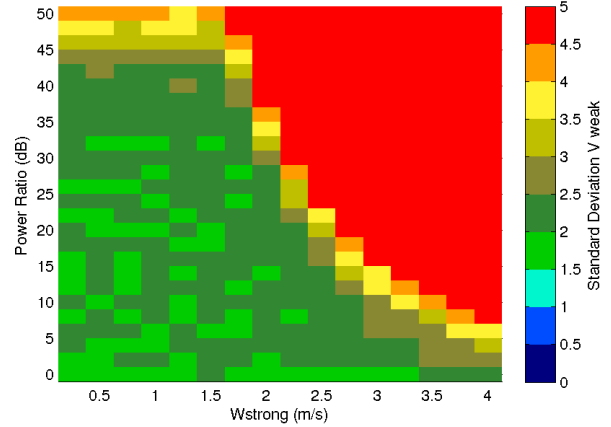


Figure 6: Standard deviation for weak trip velocity for SZ(16/128) (strong trip) SZ(15/128) (weak trip). Left: weak trip SW =  $2\text{ m s}^{-1}$ ; Right: weak trip SW =  $4\text{ m s}^{-1}$ . PRT=2 ms, 128 samples.

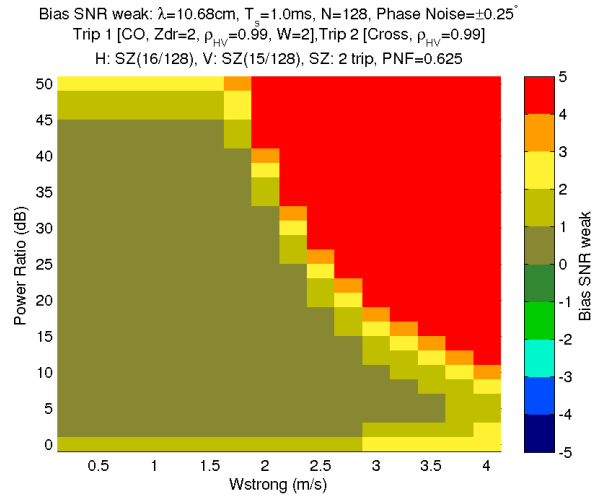


Figure 7: The bias for weak trip power (SNR) for SZ(16/128) (strong trip) SZ(15/128) (weak trip)). Weak trip  $SW=2\text{ m s}^{-1}$ . PRT=2 ms, 128 samples.

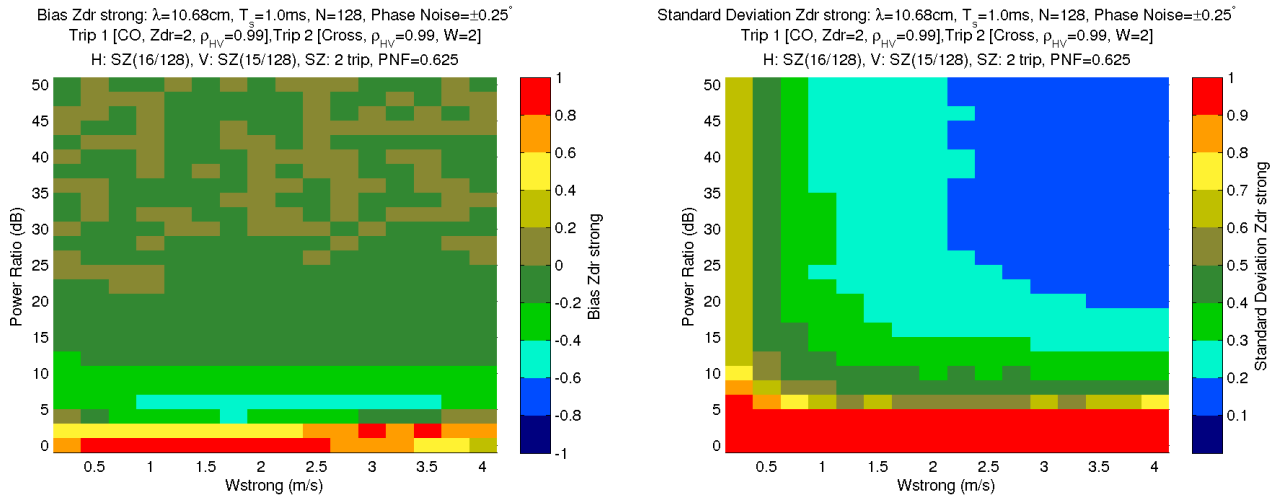


Figure 8: Strong trip  $Z_{dr}$ . Bias (left) and standard deviation (right) for SZ(16/128) (strong trip) SZ(15/128) (weak trip)). Weak trip  $SW=2\text{ m s}^{-1}$ . PRT=2 ms, 128 samples.



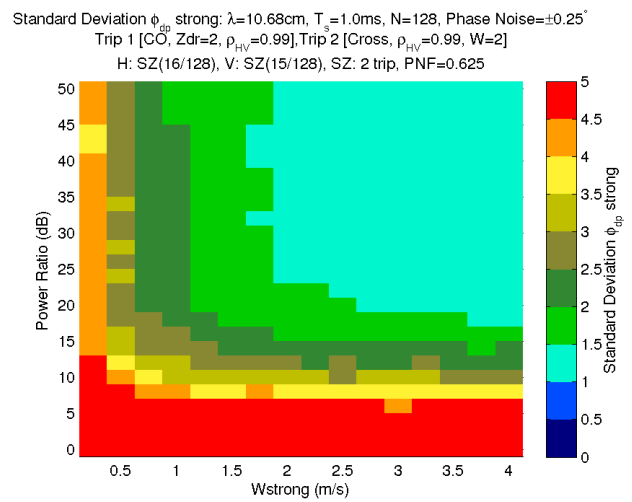
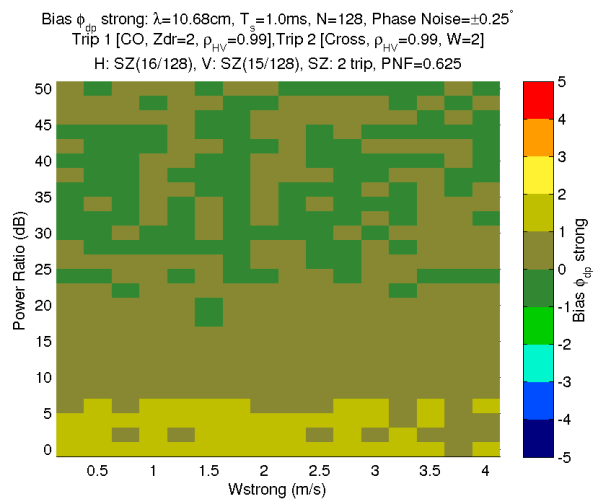


Figure 9: Strong trip  $\phi_{dp}$ . Bias (left) and standard deviation (right) for SZ(16/128) (strong trip) SZ(15/128) (weak trip). Weak trip  $SW=2\text{ m s}^{-1}$ . PRT=2 ms, 128 samples.